ResearchGate

See discussions, stats, and author profiles for this publication at: https://www.researchgate.net/publication/6907638

The Second Half of the Fourth Period of Tropomyosin Is a Key Region for Ca 2+ − Dependent Regulation of Striated Muscle Thin Filaments †

ARTICLE *in* BIOCHEMISTRY · SEPTEMBER 2006

Impact Factor: 3.02 · DOI: 10.1021/bi060963w · Source: PubMed

CITATIONS
16

READS
33

6 AUTHORS, INCLUDING:

Masao Miki
University of Fukui
91 PUBLICATIONS **1,559** CITATIONS

SEE PROFILE

Available from: Masao Miki
Retrieved on: 23 January 2016

The Second Half of the Fourth Period of Tropomyosin Is a Key Region for Ca^{2+}-Dependent Regulation of Striated Muscle Thin Filaments†

Akiko Sakuma,‡ Chieko Kimura-Sakiyama,‡ Atsuhiro Onoue,‡ Yuji Shitaka,‡ Takahisa Kusakabe,‡ and Masao Miki*,‡,§

Department of Applied Chemistry and Biotechnology, and Research and Education Program for Life Science, Fukui University, 3-9-1 Bunkyo, Fukui 910-8507, Japan

Received May 16, 2006; Revised Manuscript Received June 16, 2006

ABSTRACT: Rabbit skeletal muscle α-tropomyosin (Tm), a 284-residue dimeric coiled-coil protein, spans seven actin monomers and contains seven quasiequivalent periods. X-ray analysis of cocrystals of Tm and troponin (Tn) placed the Tn core domain near residues 150−180 of Tm. To identify the Ca^{2+}-sensitive Tn interaction site on Tm, we generated three Tm mutants to compare the consequences of sequence substitution inside and outside of the Tn core domain-binding region. Residues 152−165 and 156−162 in the second half of period 4 were replaced by corresponding residues 33−46 and 37−43 in the second half of period 1, respectively (termed mTm152−165 and mTm156−162, respectively), and residues 134−147 in the first half of period 4 were replaced with residues 15−28 in the first half of period 1 (mTm134−147). Recombinant Tms designed with an additional tripeptide, Ala-Ala-Ser, at the N-terminus were expressed in *Escherichia coli*. Both mTm152−165 and mTm156−162 suppressed the actin-activated myosin subfragment-1 Mg^{2+}-ATPase rate regardless of whether Ca^{2+} and Tn were present. On the other hand, mTm134−147 retained the normal Ca^{2+}-sensitive regulation, although the actin binding of mTm alone was significantly impaired. Differential scanning calorimetry showed that the sequence substitution in the second half of period 4 affected the thermal stability of the complete Tm molecule and also the actin-induced stabilization. These results suggest that the second half of period 4 of Tm is a key region for inducing conformational changes of the regulated thin filament required for its fully activated state.

Tropomyosin (Tm)[1] is widely distributed in all cell types, stabilizing actin filaments and modulating filament function. It is an extended α-helical coiled-coil dimer that binds end to end along the F-actin helical repeat. Its amino acid sequence consists of an integral number, six or seven in vertebrates, of quasi-repeating regions that are loosely similar in sequence, each of which contains a hypothesized actin-binding motif (for review, see ref *1*). In striated muscle, Tm in association with troponin (Tn) plays a central role in the calcium regulation of muscle contraction (*2*). Tn is an elongated complex of three proteins: TnC, TnI, and TnT. TnC, TnI, and the C-terminal region of TnT comprise the globular portion (core domain) of the Tn complex. X-ray analysis of cocrystals of Tm and Tn revealed that the Tn core domain binds to Tm near residues 150−180 (*3*). However, the residues in the 150−180 sequence involved in binding to the Tn core domain are not well-defined. The elongated N-terminal region of TnT extends along the C-terminal region of Tm to the beginning of the next Tm on the actin filament. Two regions of TnT are involved in binding to Tm. Site 1 is located on residues 71−151 (*4*), which binds Tm near its 27 C-terminal residues (*5*). Site 2 is on the C-terminal fragment, 17 residues of which are critical for the Ca^{2+}-sensitizing activity of TnT (*6, 7*). The corresponding region on Tm for site 2 is not defined.

Skeletal muscle Tm consists of seven quasi-equivalent regions, each of which contributes differentially to its regulatory function. The functions of the periodic regions in Tm have been extensively studied (*8*−*13*). Deletion of approximately half of a period or one complete period has little effect on its ability to bind actin or inhibit actin-activated myosin ATPase activity in the absence of Ca^{2+} (*8*). Deletion mutants of Tm, lacking periods 2−4 (D234Tm), 3 and 4 (D34Tm), 3−5 (D345Tm), or 4−6 (D456Tm), can bind actin, but myosin−ATPase cycling is inhibited regardless of whether Ca^{2+} is present. The Tm mutant lacking periods 2 and 3 (D23Tm) exhibited calcium-sensitive regulation of in vitro motility and actin−myosin S1 ATPase activity. The results suggest that period 4 is important for Ca^{2+}-sensitive regulation. Hitchcock-DeGregori et al. (*13*) reported that periods 4 and 5 of Tm are especially important for acto-myosin ATPase activation in the presence of Ca^{2+} and for myosin S1-induced binding of Tm to actin, respectively. Period 4 consists of residues 124−165 and period 5 of residues 166−207. The Tn core domain is located near the

† This study was performed with the Special Coordination Funds of the Ministry of Education, Culture, Sports, Science and Technology, Japan.

* To whom correspondence should be addressed. Telephone: +81-776-27-8786. Fax: +81-776-27-8747. E-mail: masao@acbio2.acbio.fukui-u.ac.jp.

‡ Department of Applied Chemistry and Biotechnology.

§ Research and Education Program for Life Science.

[1] Abbreviations: DSC, differential scanning calorimetry; DTT, dithiothreitol; Tm, tropomyosin; Tn, troponin; S1, myosin subfragment-1; PCR, polymerase chain reaction; D234Tm, rabbit Ala-Ser-αTm in which periods 2−4 have been deleted; BME, β-mercaptoethanol; wt-Tm, rabbit Ala-Ala-Ser-αTm expressed by *E. coli*.

10.1021/bi060963w CCC: $33.50 © 2006 American Chemical Society
Published on Web 07/18/2006

second half of period 4 and the first half of period 5 (residues 150−180). In the case of deletion mutant D234Tm (*10*), period 1 is connected directly to period 5, and consequently, residues 150−165 at the Tn core domain-binding region were replaced with corresponding residues 31−46 in period 1. The reasoning is that having the period 1 sequence in place of period 4 causes its loss of function. To test this hypothesis, the mutants were designed by replacing the period 4 sequence with the period 1 sequence, duplicating it. In this paper, we generated three Tm mutants in which the amino sequences inside and outside of the Tn core domain-binding region in period 4 were substituted with the corresponding sequences in period 1.

Differential scanning calorimetry (DSC) has been extensively used to study the thermal denaturation of Tm from skeletal and smooth muscles (*14*−*18*). Recently, DSC has been used to study not only the stability of Tm alone but also its specific interaction with actin filaments (*17*, *18*). In the absence of F-actin, the thermal unfolding of Tm is reversible and the heat sorption curve of Tm shows two separate calorimetric domains with maxima at ∼42 and 51 °C which correspond to the thermal stabilities of the C- and N-terminal domains of the Tm molecule, respectively. In the presence of phalloidin-stabilized F-actin which denatures at a much higher temperature than Tm, a new cooperative transition appears at 46−47 °C and completely disappears after the irreversible denaturation of F-actin. Via the measurement of temperature-dependent light scattering, the cooperative transition in the heat sorption curve by DSC corresponds well to the dissociation of Tm from F-actin (*18*). We used DSC to study the effects of segmental substitutions of Tm on its thermal stability and also its interaction with F-actin.

In this paper, we will show that the second half of period 4 of Tm is a key region for inducing conformational changes of the regulated thin filament required for its fully activated state.

MATERIALS AND METHODS

Phalloidin from *Amanita phalloides* was purchased from Sigma. All other chemicals were analytical grade.

Protein Preparation. Actin, myosin subfragment-1 (S1), and Tn were prepared from rabbit skeletal muscle as described previously (*19*−*21*). Tn was purified by DEAE-Toyopearl 650 M column chromatography (*22*). Rabbit αTm was prepared from rabbit hearts as described previously (*23*). The deletion mutant Tm (D234Tm), in which internal actin-binding pseudorepeats 2−4 had been removed, was prepared as reported previously (*10*, *24*).

Construction of Tropomyosin Mutants. Rabbit αTm cDNA was used for construction of all mutants. The cDNA was cloned into vector pET24a+ for expression in *Escherichia coli*, with the addition of oligonucleotides encoding Ala-Ala-Ser at the N-terminus of Tm (wt-Tm) (*25*). This addition can substitute for acetylation and restore actin binding ability (*26*). In the Tm mutants, mTm152−165, mTm134−147, and mTm156−162, the sequences in period 4 (residues 123−165) were substituted with the corresponding part in period 1 (residues 1−46). The Tm mutants were created using oligonucleotide-directed mutagenesis of double-stranded DNA (in pET24a+) on the basis of PCR methods. Sequences encoding mutated amino acid residues in period 4 of Tm in the plasmid were exchanged by using PCR primers. To avoid the complication that primers for mutations in period 4 have affinity for the DNA sequence in the first period, another codon encoding the same amino acid was used for the mutagenesis. PCR products were ligated to generate a circular pET24a+ plasmid. The sequences of PCR primers were as follows: 5′-TAGTTGTTTACTACGATC-CTCGGCCTCTTTCAGTTGGATCTCCT-3′ and 5′-GAG-GACGAATTAGTAAGCCTTGCCCGCAAGCTGGTCA-TCATTGAGA-3′ for mTm152−165, 5′-ACGGTCTAATG-CGTTTTCTTTTCGGCTTTCAATGACTTTCATGCCT-3′ and 5′-GCTGAACAAGCAGAAGCAGACCTGAAAGAG-GCCAAGCACATTGCTG-3′ for mTm134−147, and 5′-AAGTTGTTTAGCAATGTGCTTGGCCTCTTTCA-3′ and 5′-GAGGACGAATAGAAGAGGTGGCCCGCAAGC-3′ for mTm156−162.

The oligonucleotides used for mutagenesis were synthesized and purified by Invitrogen Life Technologies. Sequences of all mutants were confirmed by DNA sequencing (ABI Genetic Analyzer 310). Expression in BL21(DE3) cells and purification of Tm mutants were carried out as previously reported (*26*, *27*).

Protein concentrations were determined from the absorbance using extinction coefficients (0.1%): $A_{290} = 0.63$ cm^{-1} for G-actin, and $A_{280} = 0.75$ cm^{-1} for S1, 0.24 cm^{-1} for Tm and Tm mutants, 0.27 cm^{-1} for D234Tm, and 0.45 cm^{-1} for Tn. Relative molecular masses of 42 000 Da for actin, 115 000 Da for S1, 66 000 Da for Tm and Tm mutants, 37 700 Da for D234Tm, and 69 000 Da for Tn were used.

DSC Experiments. Calorimetric measurements were taken using a MicroCal model MCS differential scanning microcalorimeter with cell volumes of 1.2 mL, interfaced with a personal computer. All measurements were carried out in 20 mM Hepes (pH 7.3) containing 100 mM KCl, 2 mM $MgCl_2$, 0.1 mM $CaCl_2$, and 1 mM β-mercaptoethanol (BME) (DSC buffer), at a scanning rate of 1.0 °C/min. To split disulfide bonds between chains in the Tm homodimers, Tm was reduced for 3 h at 25 °C with 100 mM BME in the presence of 4 M guanidine-HCl and dialyzed against 10 mM Tris-HCl (pH 8.0) and 1 mM DTT. Prior to DSC experiments, all samples, including phalloidin-stabilized F-actin, Tm, and Tn, were dialyzed against the same DSC buffer solution. The final concentrations of F-actin, Tm, and Tn were 1.2, 1.0, and 1.0 mg/mL, respectively. The reversibility of the thermal transition was assessed by reheating the samples immediately after cooling them from the previous scan. The calorimetric traces were corrected for instrumental background by subtracting a scan with buffer in both cells. All calculations were carried out using Origin. The thermal stabilities of proteins were described with temperatures at maxima of the thermal transition (T_m). The calorimetric enthalpy (ΔH_{cal}) was calculated from the area under the excess heat capacity function.

ATPase Assay. The biological activity of the Tm mutant was assayed by assessing the Ca^{2+}-dependent regulation of actin-S1 ATPase activity in a fully reconstituted system. Increasing total concentrations of Tm−Tn complexes were added to samples with constant concentrations of actin (4 μM) and S1 (1 μM) in 10 mM KCl, 5 mM $MgCl_2$, 1 mM DTT, 2 mM ATP, and 20 mM MOPS (pH 7.0) and in the presence of 50 μM $CaCl_2$ (+Ca) or 1 mM EGTA (−Ca) at

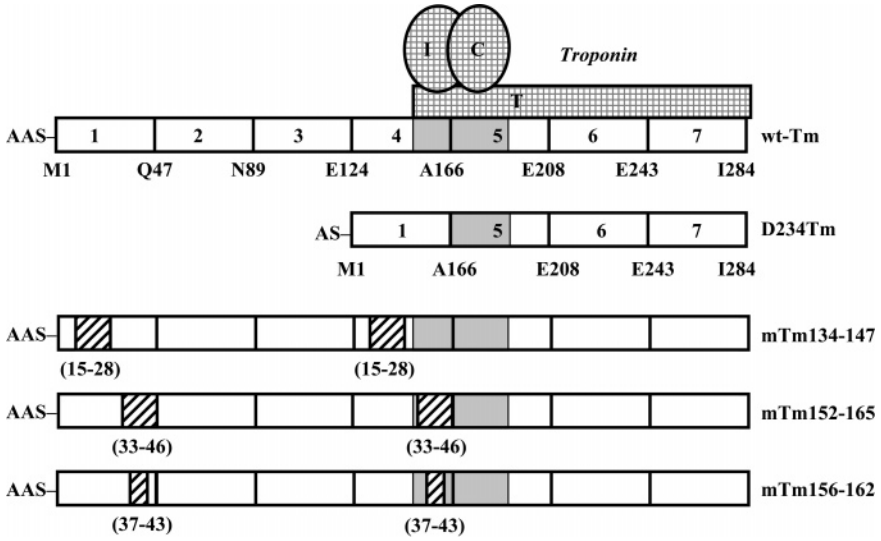

FIGURE 1: Schematic representation of the substituted amino acid residues in rabbit αTm. The Tm molecule contains seven quasi-equivalent regions, each of which contains a pair of putative actin-binding motifs. X-ray analysis of cocrystals of Tm and Tn showed that the Tn core domain binds Tm near residues 150−180 (*3*). Residues 150−180 are colored gray. In D234Tm, three of seven such periods have been deleted (*10*). In mTm134−147, mTm152−165, and mTm156−162, the mutated residues in period 4 and the corresponding residues in period 1 are cross-hatched.

25 °C. The reaction was initiated by adding S1 (total volume of the assay sample of 1.0 mL); 0.1 mL of the assay sample was removed at 2 min intervals and mixed with trichloroacetic acid (final concentration of 11.3%), and the amounts of inorganic phosphate released were determined colorimetrically according to the method of Tausky and Shorr (*28*). The rate of ATPase was determined from the slope of the amount of released phosphate versus time.

Binding Experiments. The ability of the Tm mutants to bind to actin was tested by cosedimentation assays in 20 mM Hepes (pH 7.3), 100 mM KCl, 2 mM $MgCl_2$, 0.1 mM $CaCl_2$, and 1 mM β-mercaptoethanol (BME). F-Actin (10 μM) was mixed with Tm mutants at a concentration of 0−5 μM in the presence or absence of Tn and brought up to a total volume of 200 μL. The protein mixtures were centrifuged in a Hitachi CS 100EX device with an S100AT5 rotor at 100 000 rpm for 30 min at 20 °C. Equivalent samples of supernatant and pellet were then separated by SDS−PAGE performed according to the method of Laemmli (*29*) using 12.5% acrylamide gels and stained with Coomassie G250 (Bio-Safe Coomassie; Bio-Rad). Quantification of Tm in the supernatant and pellet was carried out using an Epson GT-8700 scanner with a transparency adaptor attached to a personal computer. The scanned images were analyzed using the image software (QuantiScan, Biosoft).

RESULTS

Mutant Design. Deletion mutant D234Tm inhibits the thin filament-activated myosin-ATPase activity regardless of whether Ca^{2+} is present (*10*). In D234Tm, the sequence from period 1 is in the place of period 4, next to period 5, and consequently, a part of the Tn core domain-binding region in the second half of period 4 (residues 150−165) is deleted (Figure 1). The reasoning is that having the period 1 sequence in place of period 4 causes its loss of function. We designed the mutants to test this hypothesis by replacing the period 4 sequence with the period 1 sequence, duplicating it. Here, two Tm mutants (mTm152−165 and mTm156−162) in which 14 or 7 residues in the second half of period 4 were substituted with the corresponding residues in period 1 were generated. A mutant Tm (mTm134−147) was generated as a control, in which residues 134−147 outside of the Tn core domain-binding region were substituted with corresponding residues 15−28 in period 1. Figure 1 shows a schematic representation of the mutated sequence in period 4 with the corresponding sequence in period 1 in rabbit skeletal muscle αTm. These Tm mutants were expressed in *E. coli* as fusion proteins, having an additional tripeptide, Ala-Ala-Ser (wt-Tm, mTm134−147, mTm152−165, and mTm156−162), or dipeptide, Ala-Ser (D234Tm), at the N-terminus for sustaining the ability to bind F-actin (*26*).

Binding of Tm Mutants to F-Actin. To test the effects of mutations on the ability to bind actin, cosedimentation binding experiments were performed. Mixtures of F-actin and Tm mutants were centrifuged, and the densities of Tm bands of the supernatant and pellets on SDS gels were quantified using Image-PC (QuantiScan). Figure 2 plots the cooperative binding curves for binding of the different mTms to F-actin (filled symbols). These curves were fitted with the Hill equation, and the concentration of free Tm at which half of the actin becomes saturated ($K_{50\%}$) was determined. The $K_{50\%}$ values that were obtained were 0.15 μM for wt-Tm, 0.36 μM for mTm152−165, 0.28 μM for mTm156−162, and 3.04 μM for mTm134−147. The mutation of residues 156−162 or 152−165 slightly reduced the affinity of Tm for actin, but the mutation of residues 134−147 strongly impaired the binding ability of Tm. A cosedimentation assay for mTm134−147 was performed in the presence of the equivalent amount of Tn to Tm. The $K_{50\%}$ value for mTm134−147 in the presence of Tn (empty symbol) was 0.07 μM. The ability of mTm134−147 to bind F-actin was restored by the addition of Tn.

Ca^{2+}-Dependent Regulation of Actin−Myosin S1 ATPase. The effects of mutations on Ca^{2+}-dependent regulation of the actin−S1 MgATPase were examined. The ATPase activities of actoS1 with mTms and Tn were compared to that of

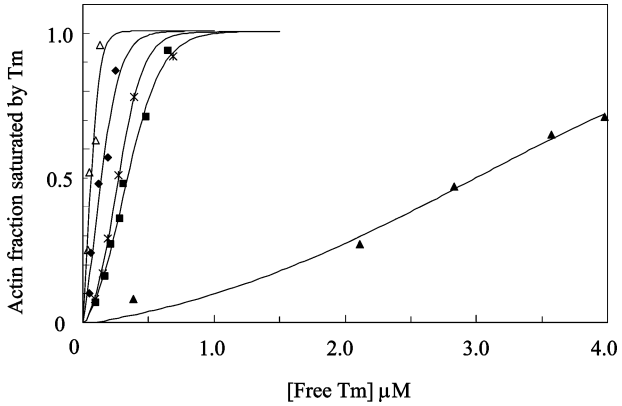

FIGURE 2: Binding of Tm mutants to actin. Tm, at concentrations ranging from 0 to 5 μM, depending on the mutants, was cosedimented with 10 μM actin in 20 mM Hepes (pH 7.3), 100 mM KCl, 2 mM $MgCl_2$, 0.1 mM $CaCl_2$, and 1 mM β-mercaptoethanol. The Tn concentration was equivalent to the Tm concentration. The curves were fitted to the data using the Hill equation. The $K_{50\%}$ values, corresponding to the Tm concentration at which half of actin becomes saturated, are 0.15 μM for wt-Tm (◆), 0.36 μM for mTm152−165 (■), 0.28 μM for mTm156−162 (∗), 3.04 μM for mTm134−147 (▲), and 0.07 μM for mTm134−147 with Tn (△).

Table 1: Ca^{2+}-Dependent Regulation of ActoS1 ATPase by mTms[a]

	with Ca^{2+}	without Ca^{2+}
rsTm	1.41 ± 0.39	0.32 ± 0.17
mTm134−147	1.36 ± 0.22	0.14 ± 0.05
mTm152−165	0.44 ± 0.22	0.19 ± 0.10
mTm156−162	0.52 ± 0.07	0.15 ± 0.03

[a] The reactions were carried out at 25 °C, with 4 μM F-actin, 1 μM rabbit skeletal S1, 0.57 μM Tm, 0.67 μM Tm, in 10 mM KCl, 5 mM $MgCl_2$, 1 mM DTT, 2 mM ATP, and 20 mM MOPS (pH 7.0) in the presence of 50 μM $CaCl_2$ (with Ca^{2+}) or 1 mM EGTA (without Ca^{2+}). A value of 1.0 is the ATPase activity of actoS1 without regulatory proteins under the same experimental conditions. The standard deviations were derived from four (mTms) or eight (rsTm) independent experiments.

actoS1 without regulatory proteins in the presence and absence of Ca^{2+} (Table 1). A value of 1.0 is the activity of actoS1 without regulatory proteins. In the absence of Ca^{2+}, all mTms, together with Tn, inhibited the actoS1 ATPase as effectively as native Tm. On the other hand, in the presence of Ca^{2+}, mTm134−147, together with Tn, activated the actoS1 ATPase as effectively as native Tm, but mTm152−165 and mTm156−162 failed to activate it even in the presence of Ca^{2+} and Tn. When the concentrations of the Tm−Tn complex were being changed, the relative activities of the actin−S1 MgATPase were measured in the presence and absence of Ca^{2+} (Figure 3). The concentration of Tn was 0.1 μM greater than that of Tm. In the absence of Ca^{2+}, increasing concentrations of all Tm mutants (mTm152−165, mTm134−147, mTm156−162, or D234Tm) inhibited actin−S1 MgATPase activity as effectively as native Tm. In the presence of Ca^{2+}, increasing concentrations of native Tm and mTm134−147 activated the actin−S1 MgATPase. On the other hand, addition of mTm152−165 and mTm156−162 reduced the activity by 76 and 66%, respectively. D234Tm reduced the activity by 93%. Thus, the sequence substitution inside the Tn core domain-binding region impaired the ability of Tm to activate the actin−S1 MgATPase in the presence of Ca^{2+} and Tn, but the substitution outside of the binding region did not.

Thermal Stability of Tm Mutants. The effects of mutations on the thermal stability of Tm were examined by using DSC. The excess heat capacity curves obtained for the Tm mutants are presented in Figure 4. The calorimetric traces were independent of heating rate (1.0 or 0.5 °C/min) and remained nearly unchanged during a second heating of the samples, suggesting that the thermal unfolding of Tm was fully reversible. The curve of wt-Tm (Figure 4A) was decomposed into two separate thermal transitions (calorimetric domain) as previously reported (*18*). There was no significant difference between wt-Tm expressed in *E. coli* and native Tm prepared from rabbit cardiac muscle. These domains with maxima at 43.5 and 51.2 °C represent 39 and 61%, respectively, of the total calorimetric enthalpy of wt-Tm. In the case of mTm134−147 (Figure 4B), two domains were also seen with maxima at 42.3 and 50.8 °C, corresponding to 36 and 64% of the total calorimetric enthalpy, respectively. However, in the case of mTm152−165, mTm156−162, and D234Tm (Figure 4C−E), only one peak was seen. These curves were deconvoluted with two Gaussian functions, and the transition temperatures of two domains were almost the same. Calorimetric parameters obtained from the DSC data are summarized in Table 2.

Thermal Stability of Tm Mutants in the Presence of Phalloidin-Stabilized F-Actin. DSC experiments with wt-Tm and phalloidin-stabilized F-actin complexes were performed under the same solvent conditions that were used for Tm alone. F-Actin stabilized with a 1.5-fold molar excess of phalloidin denatures irreversibly at 80 °C (*18*). At the first scanning, the sample was heated to 65 °C. A new highly cooperative thermal transition with a maximum at ∼47 °C appeared which corresponded to the interaction of wt-Tm with F-actin. Since excess Tm was present in the sample solution, the thermal transition of actin-free Tm was also seen in the heat sorption curves. Then, immediately after cooling to 5 °C, the sample was heated for the second time, to 90 °C (thick curve in Figure 5). The DSC profile of the second heating to 65 °C was identical to that of the first heating, and at 80 °C, a sharp transition peak was seen. It was derived from the irreversible denaturation of phalloidin-stabilized F-actin. A third heating was then carried out after the irreversible denaturation of F-actin (gray curve Figure 5). This temperature scan produced almost the same profiles for wt-Tm without F-actin (Figure 4A). The second and third DSC scans are shown in Figure 5. These results were essentially the same as those previously reported (*18*). The calorimetric enthalpy of the new cooperative thermal transition was calculated to be ∼40% of the total enthalpy of Tm under the solvent conditions described herein (Tm:actin molar ratio of 1:1.8).

To study the effects of the mutations on the interaction with F-actin, equivalent DSC experiments were carried out with Tm mutants and F-actin complexes. Figure 6A shows the first heating of the wt-Tm−F-actin complex, which was identical to the second heating to 65 °C in Figure 5. However, in the case of mTm134−147 (Figure 6B), the peak derived from the actin−Tm interaction was not seen even in the first and second heating, indicating that the affinity of mTm134−147 for actin is significantly decreased. This result is consistent with the cosedimentation experiments. In the case of mTm152−165, mTm156−162, and D234Tm (Figure 6C−E), new peaks appeared at 49−52 °C and these peaks

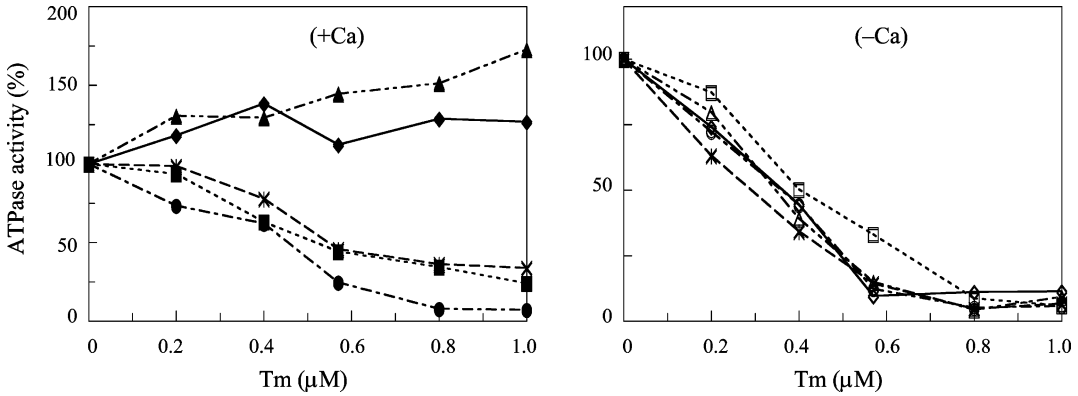

FIGURE 3: Ca^{2+} regulation of actin−myosin−S1 ATPase activity by Tm mutants with Tn: (◆ and ◇) native αTm, (■ and □) mTm152−165, (▲ and △) mTm134−147, (∗) mTm156−162, and (● and ○) D234Tm. Filled symbols (+Ca) are for measurements with 0.1 mM $CaCl_2$. Empty symbols (−Ca) are for measurements with 1 mM EGTA. The reaction conditions were 4 μM F-actin, 1 μM rabbit skeletal S1, 10 mM KCl, 5 mM $MgCl_2$, 1 mM DTT, 2 mM ATP, and 20 mM MOPS (pH 7.0) in the presence of 50 μM $CaCl_2$ (+Ca) or 1 mM EGTA (−Ca) at 25 °C. Tm concentrations ranged from 0 to 1.0 μM with Tn in 0.1 μM excess over Tm. Averaged rates from two experiments are shown.

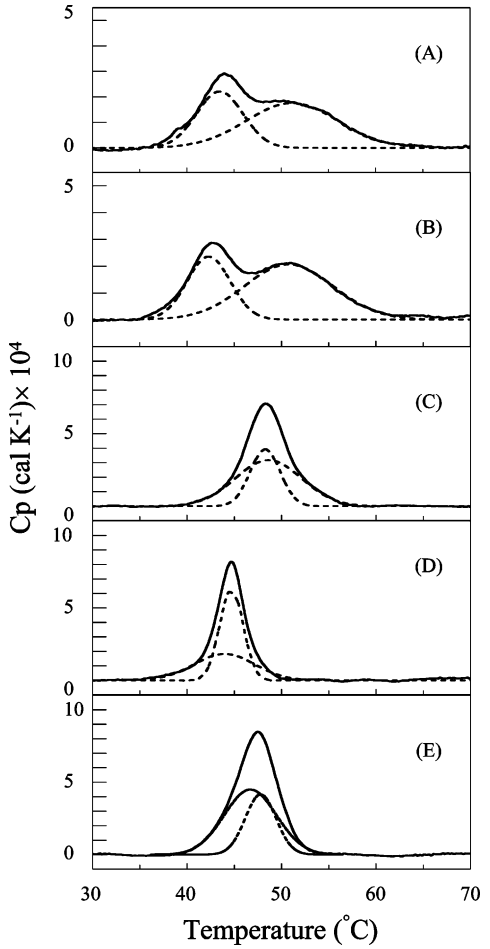

FIGURE 4: DSC scans of Tm mutants: (A) wt-Tm, (B) mTm134−147, (C) mTm152−165, (D) mTm156−162, and (E) D234Tm. The Tm concentration was 1.0 mg/mL in DSC buffer. Curves were obtained by a second heating of the same samples immediately after cooling from the first scan. The heating rate was 1.0 °C/min. Solid lines represent the experimental curves after subtraction of instrumental and chemical baselines, and dashed lines represent the individual thermal transitions obtained from fitting the data to the non-two-state model.

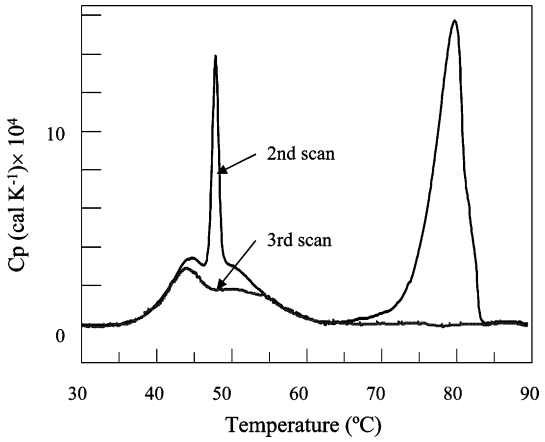

FIGURE 5: DSC scans of wt-Tm in the presence of phalloidin-stabilized F-actin. The DSC scan up to 65 °C at the second heating (thick curve) was identical to the scan obtained from the first heating. The peak at 80 °C in the second scan was derived from the denaturation of phalloidin-stabilized F-actin. After the complete denaturation of F-actin during the second heating, the third scan (gray curve) was similar to that of wt-Tm in the absence of F-actin (Figure 4A). Conditions: 1.0 mg/mL Tm and 1.2 mg/mL F-actin in DSC buffer.

Table 2: Calorimetric Parameters[a] of the Thermal Unfolding of Tm

	T_m1[b] (°C)	ΔH (%)	T_m2[b] (°C)	ΔH (%)	total ΔH_{cal}[c] (kcal/mol)
wt-αTm	43.5	39.0	51.2	61.0	193.1
mTm134−147	42.3	35.8	50.8	64.2	207.4
mTm152−165	48.3	36.0	48.6	64.0	238.2
mTm156−162	44.0	43.0	44.7	57.0	189.2
D234Tm	46.7	64.7	47.8	35.3	151.5

[a] The parameters were extracted from Figure 4. [b] The error for the given values of the transition temperature (T_m) did not exceed ±1.0 °C in two experiments. [c] The relative error of the given values of calorimetric enthalpy, ΔH_{cal}, did not exceed ±10% in two experiments.

disappeared during the third heating after the irreversible denaturation of F-actin. The concentrations of actin and Tm in DSC measurements were 29 and 15 μM (mTm152−165 and mTm156−162, respectively) and 26 μM (D234Tm). Under these conditions, only $^4/_{15}$ of Tm binds to actin. The scan curves were then analyzed with three transition components, two of which correspond to those of free Tm and one of which corresponds to the interaction with F-actin (T_m1, T_m2, and T_m3 in Table 3). Calorimetric parameters obtained from the DSC data are summarized in Table 3. Transition temperatures T_m1 and T_m2 obtained from the mixture of

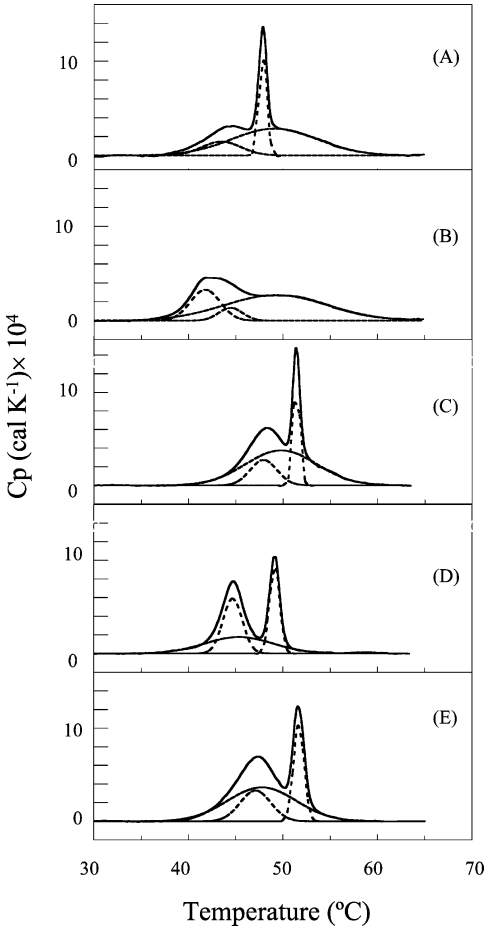

FIGURE 6: DSC scans of Tm mutants in the presence of phalloidin-stabilized F-actin: (A) wt-Tm, (B) mTm134−147, (C) mTm152−165, (D) mTm156−162, and (E) D234Tm. Solid lines represent the experimental curves after subtraction of instrumental and chemical baselines, and dashed lines represent the individual thermal transitions (calorimetric domains) obtained from fitting the data to the non-two-state model. Conditions: 1.0 mg/mL Tm and 1.2 mg/mL F-actin in DSC buffer.

F-actin and Tm (Table 3) were almost the same as those obtained for Tm alone (Table 2).

DISCUSSION

Many features of tertiary structure of α-helical coiled coils, such as Tm, have been recognized directly from primary sequence information. The α-helical coiled-coil motif is characterized by a seven-residue (so-called "heptad") repeat pattern (*a-b-c-d-e-f-g*) in which residues *a* and *d* form the hydrophobic core. Tm has an unbroken series of 40 continuous heptads and contains a relatively high frequency of Al (Ala clusters) and other small hydrophobic residues in the *a* and *d* interface positions which allow flexibility for the stable coiled-coil structure of Tm (*1*, *30*−*32*). Additional stabilization of the coiled coil is provided by salt links between residues *e* and *g* on neighboring chains, favoring a parallel in-register arrangement for two-chain molecules. Here we tested the consequences of sequence substitutions based on the primary sequence information. In Figure 7, the amino acid sequences of the substituted regions in the three Tm mutants are compared with the native αTm sequence.

mTm134−*147*. In this mutation, the segmental substitution was introduced into the outside of the Tn core domain-binding region. As expected, this mTm performed the Ca^{2+} regulation with Tn as well as wt-Tm. However, unexpectedly, the actin binding of mTm alone was significantly impaired. Singh and Hitchcock-DeGregori (*31*) reported that the core residue mutation influences the local structure and stability of Tm which is important for actin binding. The mutant Tm, in which three Ala residues of an Ala cluster were changed to canonical interface residues, A74L/A78V/A81L, exhibits an increased stability of the coiled coil, resulting in a reduction of actin affinity of >10-fold (*31*). In contrast, an Ala cluster was added in mTm134−147 where the A-D-M-Q sequence (134−144) at the *a* and *d* positions was substituted with the K-A-A-A sequence (Figure 7). The DSC scan showed that the segmental substitution did not change the thermal stability (Table 2). Therefore, the reduction in actin affinity in this mTm could not be attributed to the change in stability. On the other hand, Stewart and McLachlan (*33*, *34*) suggested that the 14 quasi-equivalent actin-binding sites are arranged in two sets of seven zones, called the α and *β* sites, and binding of Tm to actin occurs by salt linkages to basic groups on the actin surface. From the analysis of the Tm crystal structure, Phillips et al. (*35*) concluded that there are seven dominant sites roughly equivalent to the α zones of Stewart and McLachlan (the N-terminal halves of each period) that could correspond to actin contact sites. E139 and E142 are relatively regular negatively charged surface residues (positions *f* and *b*) in the fourth α zone, which are proposed to form close contacts with actin (*36*). However, these negative charges were not changed in mTm134−147 (E139D and E142E), so the reduction in actin affinity could not be attributed to a change in these surface negative charges. On the other hand, there are only four charged residues in the *a* and *d* positions, K15 (*a*), K29 (*a*), D137 (*d*), and E218 (*a*), in the amino acid sequence of rabbit skeletal αTm. Among them, K15, D137, and E218 are highly conserved (*32*). In addition, the charge alignment in residues 137−140 (D-E-E-K or -R) is highly conserved. In mTm134−147, the D-E-E-K sequence was substituted with A-L-D-R sequence and Ala134 (*a*) was substituted with a positively charged residue, K. Our results suggest that charge alignment in this conserved region (residues 137−140) in the fourth α zone is important for actin binding.

mTm152−*165 and mTm156*−*162*. In these mTms, the sequence substitutions (14 residues and their 7 central residues) were introduced into the inside of the Tn core domain-binding region. These mTms exhibited normal affinities for

Table 3: Calorimetric Parameters[a] of the Thermal Unfolding of Tm in the Presence of F-actin

	T_m1[b] (C) (°C)	ΔH (%)	T_m2[b] (N) (°C)	ΔH (%)	T_m3[b] (AT) (°C)	ΔH (%)	total ΔH_{cal}[c] (kcal/mol)
wt-αTm	43.5	14.9	49.1	63.5	47.9	21.6	280.5
mTm134−147	41.8	23.8	49.3	68.3	44.5	7.9	298.1
mTm152−165	47.9	17.5	49.8	64.0	51.4	18.6	305.3
mTm156−162	44.7	34.8	45.6	36.6	49.1	28.6	240.4
D234Tm	47.1	22.0	47.8	54.3	51.7	23.8	191.7

[a] The parameters were extracted from Figure 6. DSC scan curves were analyzed with three Gaussian distributions, two of which correspond to the free Tm and one of which corresponded to the Tm−F-actin interaction domain. [b] The values of T_m1 and T_m2 agree well with the values of free Tm shown in Table 2. The error for the T_m3 values did not exceed ±0.5 °C in two experiments. [c] The relative error for the given values of calorimetric enthalpy, ΔH_{cal}, did not exceed ±10% in two experiments.

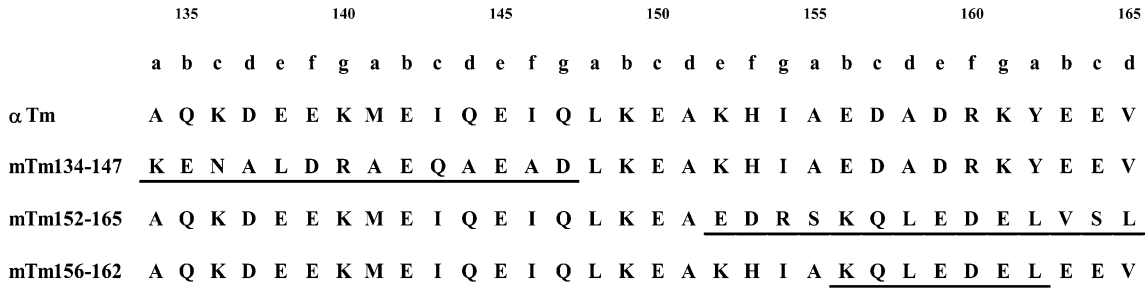

FIGURE 7: Amino acid sequences of αTm, mTm134−147, mTm152−165, and mTm156−162 in the region of residues 134−165. Mutated amino acids are underlined.

actin but did not perform the Ca^{2+} regulation, and as more Tm bound to actin in the presence of Tn, the level of actin-activated S1-ATPase (at an S1:actin molar ratio of 1:4) decreased irrespective of the Ca^{2+} concentration. This result suggests that the segment of residues 152−165 is critical for proper Ca^{2+} regulation. On the other hand, the 17 C-terminal residues of TnT, which contain six basic but no acidic residues, are critical for the Ca^{2+}-sensitizing activity of TnT (*6*, *7*). The segment of residues 152−165 on Tm appears to constitute the Ca^{2+}-sensitive TnT binding site. The sequence substitutions in mTm152−165 and mTm156−162 changed the net charge by only −2 or −1, but the alignment of these charged residues changed significantly. Most of charges at surface positions *b*, *c*, and *f* were reversed (Figure 7). Therefore, the 17 C-terminal residues of TnT could not bind correctly to mTm152−165, mTm156−162, and D234Tm, which may cause the loss of the Ca^{2+}-sensitizing regulation. This presumption is supported by the fluorescence resonance energy transfer measurements on reconstituted thin filaments (*24*, *37*, *38*). TnI and TnT in the Tn complex change their positions on the actin filament corresponding to three states of the reconstituted thin filament (relaxed, Ca^{2+}-induced or closed, and S1-induced or open states) (*24*, *37*). However, when the thin filament is reconstituted with D234Tm instead of native Tm, the Ca^{2+}-induced movement of TnT is severely impaired (*38*), although the Ca^{2+}-induced movement of TnI is normal (*24*). This deficiency of Ca^{2+}-induced movement of TnT on the mutant thin filament causes the altered S1-induced movements of TnI and TnT, and consequently, mutant thin filaments fail to activate the myosin−ATPase activity even in the presence of Ca^{2+} (*24*, *38*).

Residues 47−165 have been deleted from the amino acid sequence of D234Tm (Figure 1). The sequence substitution was performed in D234Tm for the purpose of reconstructing the Tn core domain-binding region. Residues 31−46 in D234Tm were replaced with residues 150−165 of αTm. This mutant Tm (D234Tm31−46) has residues 1−30 and 150−284. Thus, the Tn core domain-binding region (residues 150−165) was restored. Using D234Tm31−46, we performed ATPase measurements under the same conditions that are shown in Figure 3. D234Tm31−46 yielded results similar to those of D234Tm (data not shown). It did not recover the ability of Ca^{2+} regulation, indicating that the recovery of the Tn core domain-binding site (residues 150−165) on D234Tm is not enough to change the conformation of the regulated actin filament from inactive to active. After the Ca^{2+}-sensitizing interaction between the C-terminal region of TnT and residues 150−165 on Tm, an induced conformational change in the Tn−Tm−actin complex may be required for the fully activated state.

DSC measurements suggested that the sequence substitutions of the middle segment (residues 152−165) affected the thermal stability of the complete Tm molecule. The DSC scan curve of wt-Tm shows two separate peaks at ∼42 and 51 °C which correspond to the thermal stability of the C-terminal part and the N-terminal part, respectively (*14*, *18*). The DSC scans of mTm152−165 and mTm156−162 have only a single peak in the heat sorption curves. Sequence substitutions (residues 152−165 and 156−162) seem to increase and decrease the thermal stabilities of the C- and N-terminal parts, respectively. It was rather surprising that the DSC scan of D234Tm, in which most of the N-terminal part was deleted, showed almost the same curve as that of mTm152−165. The transition temperature of mTm152−165 was ∼4 °C higher than that of mTm156−162. This could be attributed to a salt linkage between side chains in the *g* position (154) and *e* position (159) formed in mTm152−165 (R-E), but not in mTm156−162 (I-E). The Ala clusters, interface alanines of the Tm coiled coil, are closely related to the local structure and stability (*30*, *31*). The mutation of the Ala cluster (residues 74, 78, and 81) to L, V, and L, respectively, in the second half of period 2 strongly increased the thermal stability of the N-terminal part but did not change the stability of the C-terminal part (*31*). The Ala cluster (residues 151, 155, and 158) was replaced with A, S, and L, respectively, in mTm152−165 and A, A, and L, respectively, in mTm156−162 (Figure 7). In contrast to the mutation in the Ala cluster in the second half of period 2, the mutation in the second half of period 4 affects the thermal stability of the complete Tm molecule.

This sequence substitution modulates not only the thermal stability but also the actin−Tm interaction. DSC scans of D234Tm, mTm152−165, and mTm156−162 in the presence of phalloidin-stabilized F-actin display a new, highly cooperative thermal transition corresponding to the interaction with F-actin, as previously reported for native and wild-type Tm (*17*, *18*). The transition temperatures of actin-induced stabilization (T_m3) of D234Tm, mTm152−165, and mTm156−162 were significantly higher than those (T_m1 and T_m2) of free Tm, suggesting that thermal denaturation of actin-bound Tm occurs only upon its cooperative dissociation from F-actin. On the other hand, the actin−Tm transition temperatures (T_m3) of D234Tm, mTm152−165, and mTm156−162 were significantly higher than that of wt-Tm (Table 3), indicating that the interaction of these mTms with actin is thermally more resistant. The actin−Tm transition temperatures are not directly related to the actin affinity constants

determined by cosedimentation assays at the constant temperature. The actin affinities determined by cosedimentation assays for D234Tm (*10*), mTm152−165, and mTm156−162 (Figure 2) were slightly lower than those of wt-Tm, but those Tm mutants have higher transition temperatures for actin-induced stabilization than wt-Tm. One explanation for this phenomenon may be that the destabilization in the C-terminal domain of Tm causes its dissociation from actin (*18*). The thermal stability of the C-terminal domain was greater in mTms than in wt-Tm, so mTms exhibited higher actin−Tm transition temperatures than wt-Tm. An alternative explanation is that hydrophobic bonds are stabilized by an increase in temperature. These mTms, due to a conformational change, use more hydrophobic but fewer ionic bonds for interaction with actin than wt-Tm, resulting in the slightly lower actin affinities but higher transition temperatures of actin-induced stabilization.

At present, it is not clear how the altered thermal stability of mTms relates to the loss of Ca^{2+}-sensitive regulation, since the DSC measurements were carried out in the absence of Tn. In future studies, DSC measurements in the presence of Tn with and without Ca^{2+} will be necessary. However, these DSC measurements show that the conformational change in the middle segment (residues 152−165) of the Tm molecule could modulate not only the stability of the complete Tm molecule but also the actin−Tm interaction, suggesting that a conformational change in this region of Tm may be a key event for myosin-dependent activation of the regulated actin filament in the presence of Ca^{2+}.

ACKNOWLEDGMENT

We thank Dr. Y. Nitanai for discussions about the amino acid sequence of Tm and Drs. S. E. Hitchcock-DeGregori and C. G. dos Remedios for comments on the manuscript.

REFERENCES

1. Perry, S. V. (2001) Vertebrate tropomyosin: Distribution, properties and function, *J. Muscle Res. Cell Motil. 22*, 5−49.
2. Ebashi, S., Endo, M., and Ohtsuki, I. (1969) Control of muscle contraction, *Q. Rev. Biophys. 2*, 351−384.
3. White, S. P., Cohen, C., and Phillips, G. N., Jr. (1987) Structure of co-crystals of tropomyosin and troponin, *Nature 325*, 826−828.
4. Jackson, P., Amphlett, G. W., and Perry, S. V. (1975) The primary structure of troponin T and the interaction with tropomyosin, *Biochem. J. 151*, 85−97.
5. Hammell, R. L., and Hitchcock-DeGregori, S. E. (1996) Mapping the functional domains within the carboxyl terminus of α-tropomyosin encoded by the alternatively spliced ninth exon, *J. Biol. Chem. 271*, 4236−4242.
6. Ohtsuki, I., Yamamoto, K., and Hashimoto, K. (1981) Effect of two C-terminal side chymotryptic troponin T subfragments on the Ca^{2+} sensitivity of superprecipitation and ATPase activities of actomyosin, *J. Biochem. 90*, 259−261.
7. Onoyama, Y., and Ohtsuki, I. (1986) Effect of chymotryptic troponin T subfragments on the calcium ion-sensitivity of ATPase and superprecipitation of actomyosin, *J. Biochem. 100*, 517−519.
8. Hitchcock-DeGregori, S. E., and Varnell, T. A. (1990) Tropomyosin has discrete actin-binding sites with sevenfold and fourteenfold periodicities, *J. Mol. Biol. 214*, 885−896.
9. Hitchcock-DeGregori, S. E., and An, Y. (1996) Integral repeats and a continuous coiled coil are required for binding of striated muscle tropomyosin to the regulated actin filament, *J. Biol. Chem. 271*, 3600−3603.
10. Landis, C. A., Bobkova, A., Homsher, E., and Tobacman, L. S. (1997) The active state of the thin filament is destabilized by an internal deletion in tropomyosin, *J. Biol. Chem. 272*, 14051−14056.
11. Landis, C. A., Back, N., Homsher, E., and Tobacman, L. S. (1999) Effects of tropomyosin internal deletions on thin filament function, *J. Biol. Chem. 274*, 31279−31285.
12. Hitchcock-DeGregori, S. E., Song, Y., and Moraczewska, J. (2001) Importance of internal regions and the overall length of tropomyosin for actin binding and regulatory function, *Biochemistry 40*, 2104−2112.
13. Hitchcock-DeGregori, S. E., Song, Y., and Greenfield, N. J. (2002) Functions of tropomyosin's periodic repeats, *Biochemistry 41*, 15036−15044.
14. Williams, D. L., Jr., and Swenson, C. A. (1981) Tropomyosin stability: Assignment of thermally induced conformational transitions to separate regions of the molecule, *Biochemistry 20*, 3856−3864.
15. Potekhin, S. A., and Privalov, P. L. (1982) Co-operative blocks in tropomyosin, *J. Mol. Biol. 159*, 519−535.
16. O'Brien, R., Sturtevant, J. M., Wrabl, J., Holtzer, M. E., and Holtzer, A. (1996) A scanning calorimetric study of unfolding equilibria in homodimeric chicken gizzard tropomyosins, *Biophys. J. 70*, 2403−2407.
17. Levitsky, D. I., Rostkova, E. V., Orlov, V. N., Nikolaeva, O. P., Moiseeva, L. N., Teplova, M. V., and Gusev, N. B. (1900) Complexes of smooth muscle tropomyosin with F-actin studied by differential scanning calorimetry, *Eur. J. Biochem. 267*, 1869−1877.
18. Kremneva, E., Boussouf, S., Nikolaeva, O., Maytum, R., Geeves, M. A., and Levitsky, D. I. (2004) Effects of two familial hypertrophic cardiomyopathy mutations in α-tropomyosin, Asp175Asn and Glu180Gly, on the thermal unfolding of actin-bound tropomyosin, *Biophys. J. 87*, 3922−3933.
19. Spudich, J. A., and Watt, S. (1971) The regulation of rabbit skeletal muscle contraction. I. Biochemical studies of the interaction of the tropomyosin-troponin complex with actin and the proteolytic fragments of myosin, *J. Biol. Chem. 246*, 4866−4871.
20. Weeds, A. G., and Taylor, R. S. (1975) Studies on the chymotryptic digestion of myosin. Effects of divalent cations on proteolytic susceptibility, *Nature 257*, 54−56.
21. Ebashi, S., Wakabayashi, T., and Ebashi, F. (1971) Troponin and its components, *J. Biochem. 69*, 441−445.
22. Ojima, T., and Nishita, K. (1988) Separation of akazara scallop and rabbit troponin components by a single-step chromatography on CM-Toyopearl, *J. Biochem. 104*, 9−11.
23. Miki, M. (1990) Resonance energy transfer between points in a reconstituted skeletal muscle thin filament, *Eur. J. Biochem. 187*, 155−162.
24. Hai, H., Sano, K.-I., Maeda, K., Maéda, Y., and Miki, M. (2002) Ca^{2+}-induced conformational change of reconstituted skeletal muscle thin filaments with an internal deletion mutant D234-tropomyosin observed by fluorescence energy transfer spectroscopy: Structural evidence for three states of thin filament, *J. Biochem. 131*, 407−418.
25. Miki, M., Hai, H., Saeki, K., Shitaka, Y., Sano, K.-I., Maéda, Y., and Wakabayashi, T. (2004) Fluorescence resonance energy transfer between points on actin and the C-terminal region of tropomyosin in skeletal muscle thin filaments, *J. Biochem. 136*, 39−47.
26. Monteiro, P. B., Lataro, R. C., Ferro, J. A., and Reinach, F. C. (1994) Functional α-tropomyosin produced in *Escherichia coli*. A dipeptide extension can substitute the amino-terminal acetyl group, *J. Biol. Chem. 269*, 10461−10466.
27. Kluwe, L., Maeda, K., Miegel, A., Fujita-Becker, S., Maéda, Y., Talbo, G., Houthaeve, T., and Kellner, R. (1995) Rabbit skeletal muscle alpha alpha-tropomyosin expressed in baculovirus-infected insect cells possesses the authentic N-terminus structure and functions, *J. Muscle Res. Cell Motil. 16*, 103−110.
28. Tausky, H. H., and Shorr, E. (1953) A microcolorimetric method for the determination of inorganic phosphorus, *J. Biol. Chem. 202*, 675−685.
29. Laemmli, U. K. (1970) Cleavage of structural proteins during the assembly of the head of bacteriophage T4, *Nature 227*, 680−685.
30. Brown, J. H., Kim, K.-H., Jun, G., Greenfield, N. J., Dominguez, R., Volkmann, N., Hitchcock-DeGregori, S. E., and Cohen, C. (2001) Deciphering the design of the tropomyosin molecule, *Proc. Natl. Acad. Sci. U.S.A. 98*, 8496−8501.
31. Singh, A., and Hitchcock-DeGregori, S. E. (2003) Local destabilization of the tropomyosin coiled coil gives the molecular flexibility required for actin binding, *Biochemistry 42*, 14114−14121.

32. Lu, S. M., and Hodge, R. S. (2004) Defining the minimum size of a hydrophobic cluster in two-stranded α-helical coiled-coils: Effects on protein stability, *Protein Sci*. *13*, 714−726.
33. Stewart, M., and McLachlan, A. D. (1975) Fourteen actin-binding sites on tropomyosin, *Nature 257*, 331−333.
34. McLachlan, A. D., and Stewart, M. (1976) The 14-fold periodicity in α-tropomyosin and the interaction with actin, *J. Mol. Biol. 103*, 271−298.
35. Phillips, G. N., Jr., Filler, J. P., and Cohen, C. (1986) Tropomyosin crystal structure and muscle regulation, *J. Mol. Biol*. *192*, 111−131.
36. Brown, J. H., Zhou, Z., Reshetnikova, L., Robinson, H., Yammani, R. D., Tobacman, L. S., and Cohen, C. (2005) Structure of the mid-region of tropomyosin: Bending and binding sites for actin, *Proc. Natl. Acad. Sci. U.S.A. 102*, 18878−18883.
37. Kimura, C., Maeda, K., Maéda, Y., and Miki, M. (2002) Ca^{2+}- and S1-induced movement of troponin T on reconstituted skeletal muscle thin filaments observed by fluorescence energy transfer spectroscopy, *J. Biochem. 132*, 93−102.
38. Kimura, C., Maeda, K., Hai, H., and Miki, M. (2002) Ca^{2+}- and S1-induced movement of troponin T on mutant thin filaments reconstituted with functionally deficient mutant tropomyosin, *J. Biochem*. *132*, 345−352.

BI060963W